IEEE Access
Multidisciplinary | Rapid Review | Open Access Journal

Received January 8, 2021, accepted February 1, 2021, date of publication February 4, 2021, date of current version July 14, 2021.

Digital Object Identifier 10.1109/ACCESS.2021.3057162

Robust Current Control of Voice Coil Motor in Tip-Tilt Mirror Based on Disturbance Observer Framework

ZONGQI NING[1,2,3], YAO MAO[1,2,3], (Member, IEEE), YONGMEI HUANG[1,2,3], AND CHUNMING GAO[4]
[1]Institute of Optics and Electronics, Chinese Academy of Sciences, Chengdu 610209, China
[2]Key Laboratory of Optical Engineering, Chinese Academy of Sciences, Chengdu 610209, China
[3]University of Chinese Academy of Sciences, Beijing 100039, China
[4]University of Electronic Science and Technology of China, Chengdu 610054, China

Corresponding author: Yongmei Huang (huangym@ioe.ac.cn)

This work was supported by the National Key Research and Development Program of China under Grant 2017YFB1103002.

ABSTRACT In this paper, a control methodology based on the disturbance observer (DOB) framework is proposed to improve the current dynamic characteristic and the robustness of the voice coil motor (VCM) in the tip-tilt mirror. It is shown that the open-loop current characteristic is a third-order plant, which is influenced obviously by both the electrical and mechanical uncertainties under different environment temperatures. Although the traditional PID control is helpful to improve the current dynamics, it is not able to provide enough robustness. Therefore, a new control methodology based on DOB is proposed. The plant model is simplified from third-order to first-order by considering the back-electromotive force (EMF) as the disturbance. The perturbation of the electrical parameters is compensated by the inner-loop of the DOB framework, and the perturbation of the mechanical parameters is compensated by suppressing the back-EMF. Moreover, new sufficient conditions for robust stability are presented in the control method based on H_∞ algorithm. Compared with the traditional researches, the upper bound of the uncertainties is calculated directly in this paper. Therefore, the ranges of the electrical parameters are very clear according to the Q-filter. Based on the stability conditions, new design guidelines for the DOB-based robust current control for induction motor are also presented. Experiment results are given to show the design details and the superiority of the proposed control method.

INDEX TERMS Tip-tilt mirror, voice coil motor, disturbance observer control, robustness.

I. INTRODUCTION

Tip-tilt mirror is one of the key instruments with high accuracy and dynamics to compensate structure vibrations in astronomical telescopes, adaptive optics and FSO communications [1], [2]. The tip-tilt mirror is often driven by the assembled VCMs, which have the advantage of compact size, light weight and high position precision [3], [4]. The dynamic characteristic of the motor current, which control the trust directly, is crucial for the tip-tilt mirror to achieve high accuracy and high-response speed. Optimal design methods for VCM are discussed in the literature [5], [6]. Moreover, since the open-loop current characteristic of VCM often has a phase delay and influenced by the back-EMF, the traditional PID control is widely used in the current control of VCM [7], [8] to improve the current dynamics.

However, as the application of the tip-tilt mirror has been expanded to aerospace, the current control of the VCM faces the challenge of thermal issues. As the environment temperature changed sharply, both the electrical and mechanical characteristics of the mirror are influenced, which may cause obvious uncertainties of the open-loop current characteristic. Although the robustness of the current control can be achieved more or less by PID controller, its effect is limited by the issues of stability and the sensor noises. Till now, few research has paid attention to the temperature influence on the VCM and the robust control strategy on its current performance.

DOB has been one of the most important tools to enhance the robustness and suppress disturbance since it was proposed

The associate editor coordinating the review of this manuscript and approving it for publication was Paolo Giangrande.

by Ohnishi in 1983. In the DOB-based robust control, disturbances are estimated by the nominal model of plant, and the robustness is achieved by feed-backing the estimations of disturbances. A widely used DOB framework consists of an inner-loop and an outer-loop, which is of the advantage that the control system can be independently adjusted by tuning DOB and the performance controller in the inner and outer loops, respectively [9]–[12]. The convenience of the this kind of DOB framework has been verified in many areas such as robust motion control [13]–[16], DC-bus voltage control [17], and temperature control [18].

The DOB control method has also been widely used in the current control of induction motors [19]–[23].For example, a new method is provided to improve the gain and phase margin of the DOB system in [21]. Moreover, investigation is made on the DOB method in the predictive current control in [22]. Also, a novel sliding-mode current control law with a disturbance observer is proposed for current regulation of induction motors in [23]. However, few of them has a synthetical discussion on the robust stability of the DOB method in the current control of induction motors.

In fact, since the uncertainty of the plant, the analysis on the stability of the DOB framework with an inner-loop and an outer-loop is difficult. Since the dynamics of the Q-filter is limited by constraints such as measurement noises [24] and water-bed effect, the characteristic polynomial of the DOB control method is influenced by the Q-filter, unstructured uncertainties, nominal plant model, and outer-loop controller [25]. Therefore, parameters design is usually complicated considering the robust stability and highly depends on the personal experience.

In this paper, the open-loop current characteristic of the VCM in the tip-tilt mirror is analyzed and the influence of the environment temperature on the current dynamics is presented. It is shown that the open-loop current characteristic is a third-order plant, which is not only influenced by electrical parameter uncertainties but also by mechanical parameters uncertainties. Then the control methodology based on DOB framework is proposed to improve both the current dynamics as well as robustness. By considering the back-EMF as the disturbance, the plant model is simplified and the mechanical parameters' perturbation is suppressed. Moreover, new sufficient conditions for the robust stability based on H_∞ algorithm are presented, which is suitable for the DOB-based robust current control of induction motors. Compared with traditional H_∞ algorithm [26]–[30], the upper bound of the uncertainty is calculated directly, so that the ranges of different electrical parameters of the VCM are very clear for the robust stability. Experiment results show that as the environment temperature changes, the robustness of the current control is highly improved by the proposed methodology comparing with the traditional PID control.

The rest of paper is organized as follow. Section II introduces the tip-tilt mirror and the problem on its robust current control. The robust current control system based on DOB framework is proposed in Section III. In Section IV the robust stability conditions are newly presented. In Section V, the design details and experiment results are given to show the superiority of the proposed tragedy to improve the robustness of the VCM current control. Finally, some concluding remarks are given in Section VI.

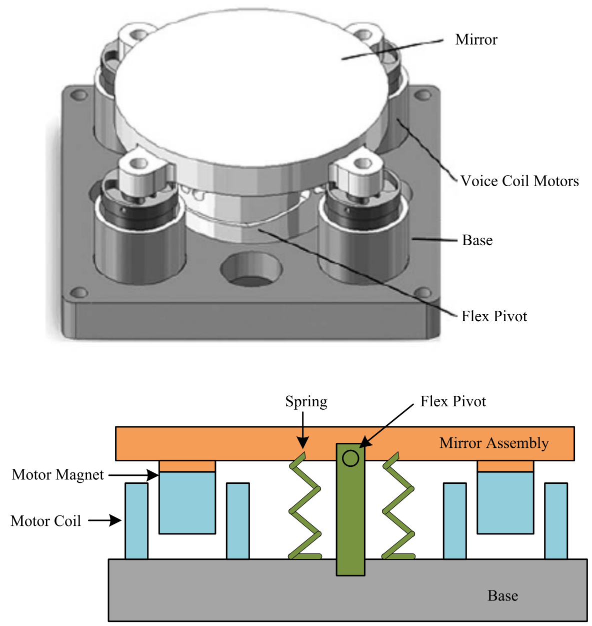

FIGURE 1. Architecture of the tip-tilt mirror driven by VCMs.

II. OPEN-LOOP CURRENT CHARACTERISTIC AND THE TEMPERATURE INFLUENCE

The general architecture of the tip-tilt mirror comprises of a mirror subassembly that is pivotally coupled to a fixed base. Four voice coil motors with primary and redundant windings are mechanically attached to the fixed base as well. The motors apply torque directly to the mirror subassembly, thereby acting like a counter-balance which helps cancel out the exported forces and torques caused by the structure vibrations. Springs are used to connect the mirror subassembly and the fixed base, so that the mirror can be fixed when the motors are not on power. Fig. 1 shows the architecture of the tip-tilt mirror.

Consider the tip-tilt mirror is controlled by the power amplifier, the output voltage of which is represented as u. The block diagram of the motor's open-loop current is depicted in Fig. 2. L and R represent the equivalent inductance and resistance of the coil winding. K_t, K_b, K_f and J are the trust constant, EMF constant, friction constant and the mass of the mirror subassembly, respectively. K_d is the spring constant. Signals r, i E_b, v and p represent the reference signal, motor current, voltage of back-EMF, velocity and position of the motor, respectively.

Let $T_{iu\_open}(s)$ represent the open-loop current characteristic of the VCM, which is the transfer function from u to i,

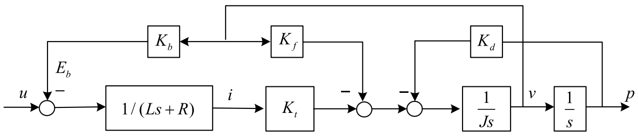

FIGURE 2. Block diagram of open-loop current control of the VCM in the tip-tilt mirror.

then from Fig. 1, $T_{iu\_open}(s)$ is computed as:

$$T_{iu\_open}(s) = \frac{Js^2+K_fs+K_d}{JLs^3+(JR+K_fL)s^2+(K_fR+C_mK_b+K_dL)s+K_dR}. \quad (1)$$

According to the polynomial theorem, $T_{iu\_open}(s)$ can be represented as:

$$T_{iu\_open}(s) = \frac{1}{(s+a_0)}\frac{Js^2+K_fs+K_d}{a_1s^2+a_2s+a_3}, \quad (2)$$

where

$$\begin{cases} a_1 = JL \\ JLa_0 + a_2 = JR + K_fL \\ a_0a_2 + a_3 = K_fR + C_mK_b + K_dL \\ a_0a_3 = K_dR. \end{cases} \quad (3)$$

It is shown that the dynamics of the VCM motor current are influenced by the phase delay and oscillation. Such an impact is not only caused by the electrical parameters of the VCM, but also by the mechanical parameters of the tip-tilt mirror because of the back-EMF. Since phase delay causes decline on the response speed and the oscillation impacts on the control accuracy of the trust, there is a demand on suppressing the phase delay and oscillation of the current dynamics.

Fig. 3 shows the test results of the open-loop current characteristic of the VCM under different temperatures. It is shown that when the environment temperature changes from $-45°C$ to $125°C$, the open-loop current is with obvious uncertainties. Thus, the control method with high robustness is required to improve the current dynamic characteristic.

III. ROBUST CURRENT CONTROL BASED ON THE DOB FRAMEWORK

This section presents the robust current control of the VCM based on the DOB framework, as shown in Fig. 4. The purpose of the control is to compensate the phase delay and oscillation of the current as well as improve the robustness of the current control system. The DOB framework consists of an inner disturbance observer loop (inner-loop) and a main feedback control loop (outer-loop). $C(s)$, $P_n(s)$ and $Q(s)$ represent the performance controller, nominal plant model and the Q-filter, respectively. q and u' represents the output signal of the performance controller and the input voltage of the VCM, respectively.

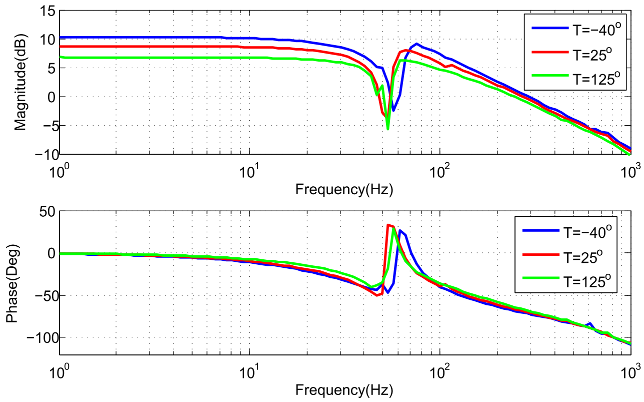

FIGURE 3. Experiment results of $T_{iu\_open}(s)$ of a VCM motor under different environment temperatures.

From Fig. 4, the plant of the system is the open-loop current characteristic of the VCM. Consider that the plant is third-order and that both the electrical and mechanical parameters of the tip-tilt motor are uncertain under different temperatures, the discussion on the robustness is difficult based on Fig. 4. As discussed in last section, the effect of mechanism on the current is caused by the back-EMF. Therefore, by considering the $E_b(s)$ as the external disturbance [8], the control system can be simplified as shown in Fig. 5.

$P(s)$ represents the transfer function from u' to i, which is computed as

$$P(s) = \frac{1}{Ls+R}. \quad (4)$$

$\Delta W(s)$ represents the uncertainties of $P(s)$. The relationship between $P(s)$ and $P_n(s)$ is described as

$$P(s) = P_n(s)(1 + \Delta W(s)). \quad (5)$$

$E_b(s)$ is computed as

$$E_b(s) = \frac{K_bK_ts}{Js^2+K_fs+K_d}i(s). \quad (6)$$

Thus, the robust control of $T_{iu\_open}(s)$ is transferred to issues of disturbance rejection of $E_b(s)$ and robust control of the plant $P(s)$. The influence of the mechanism and mechanical uncertainties are suppressed by the disturbance rejection of $E_b(s)$. The current characteristic of the control system are decided by the robust control of $P(s)$, which only consists of electrical parameters L and R. Hence, only the uncertainties of L and R should be considered in the following discussion.

From Fig. 5, the current dynamics i is computed as:

$$i(s) = T_{ir}(s)i(s) + T_{ie}(s)E_b(s). \quad (7)$$

where

$$T_{ir}(s) = \frac{(1+\Delta W)CP_n}{1+(1+\Delta W)CP_n+\Delta WQ}, \quad (8)$$

$$T_{ie}(s) = -\frac{(1+\Delta W)P_n(1-Q)}{1+(1+\Delta W)CP_n+\Delta WQ}. \quad (9)$$

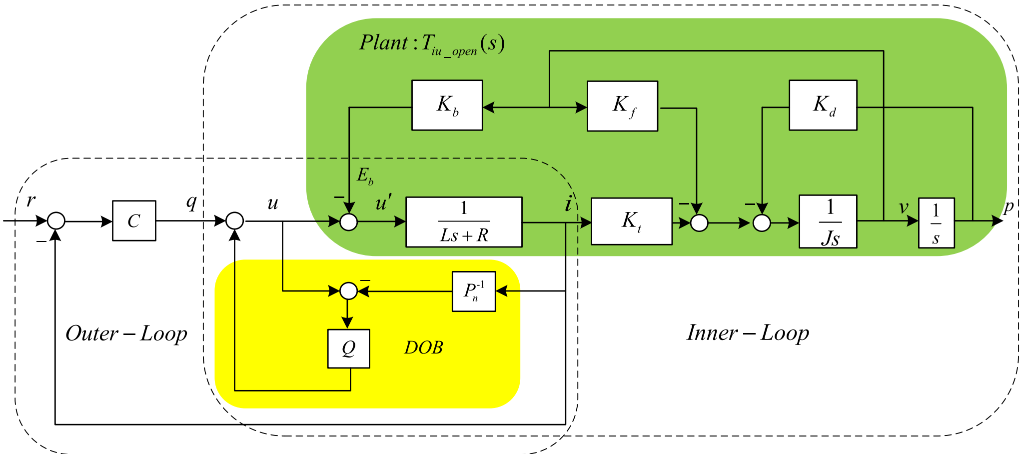

FIGURE 4. Block diagram of the robust current control of VCM in the tip-tilt mirror based on DOB framework.

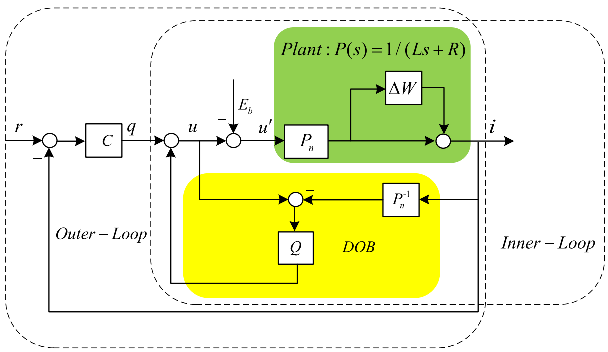

FIGURE 5. Block diagram of the simplified robust current control based on DOB framework.

If $Q(s) = 1$, then we have:

$$T_{ir}(s) = \frac{CP_n}{1 + CP_n}\Big|_{Q=1}, \tag{10}$$

$$T_{ie}(s) = 0\Big|_{Q=1}. \tag{11}$$

Equation (10) and (11) show that when $Q(s) = 1$, the current characteristic of the outer-loop is only decided by the nominal plant model and the performance controller, which is the same with the traditional closed-loop control. Therefore, the phase delay and oscillation of the open-loop current is compensated. Moreover, since the effect of $E_b(s)$ and $\Delta W(s)$ is suppressed by the DOB control method, the robustness of the system is achieved.

It should be mentioned that the Q-filter cannot be equal with the constant one in practical. Usually, it is designed as a low-pass filter considering the effect of measurement noises, water effect and other constrains. As a result, the stability, robustness and the dynamic performance of the VCM current are influenced by the Q-filter, nominal plant model, system uncertainties and the performance controller. Therefore, sufficient conditions on the robust stability are demanded.

IV. ANALYSIS ON THE ROBUST STABILITY

This section presents the new sufficient conditions for the robust stability of the current control of VCM based on the DOB control method. The conditions are convenience for practical application because the relationship between the Q-filter and electrical parameter of the motor is established.

To begin with the further discussion, the following assumption is introduced which has an agreement with the practical situation of the VCM.

Assumption 1: It is assumed that the range of uncertainties of the VCM can be acquired by testing or other methods, which is represented as:

$$L_1 \leq L \leq L_2, R_1 \leq R \leq R_2. \tag{12}$$

where L_1, L_2, R_1 and R_2 are positive real numbers. $P_n(s)$ belongs to

$$P_n(s) = \frac{1}{L_n s + R_n}, \tag{13}$$

where L_n and R_n are real positive numbers.

A. THE GENERAL SUFFICIENT CONDITIONS FOR ROBUST STABILITY

From Fig. 5, the characteristic polynomial $\delta(s)$ is computed as:

$$\delta(s) = 1 + (1 + \Delta W)CP_n + \Delta WQ, \tag{14}$$

which can be re-written as:

$$\delta(s) = (1 + P_nC)(1 + \Delta WQ_T), \tag{15}$$

where

$$Q_T = \frac{P_nC + Q}{1 + P_nC}. \tag{16}$$

Lemma 1: Assume that $\|\Delta W\|_\infty \leq \gamma$, where γ is the upper bound on the uncertainties of the plant, the system is robustly stable if the following two conditions hold.

1) $1 + P_nC$ is Hurwitz;

2) $\|Q_T\|_\infty < 1/\gamma$.

Proof:

Since

$$\|\Delta W Q_T\|_\infty \leq \|\Delta W\|_\infty \cdot \|Q_T\|_\infty, \tag{17}$$

if the condition 2) is satisfied, then

$$\|\Delta W Q_T\|_\infty < 1. \tag{18}$$

Then we have

$$1+\Delta W Q_T > 0. \tag{19}$$

According to (15), all the roots of the $\delta(s)$ are decided by the polynomial $1 + P_n C$. So if $1 + P_n C$ is Hurwitz, there is no RHP root of $\delta(s)$ and the control system is robustly stable. Thus, Lemma 1 is proved.

Condition 1) regulates the design of $C(s)$ in the DOB framework. As the nominal plant model $P_n(s)$ is selected, it is very easy to design $C(s)$ according to demand of the current dynamics.

Condition 2) indicates that the Q-filter design is limited by the upper bound of the uncertainties. Similar conditions are also given in the previous works [26]–[30]. However, such kind of condition is not clear enough for the application in the practical system. This is because γ can neither be found in the manual nor be tested directly in the control system. Therefore, it is beneficial if the condition 2) is transferred to a relationship between the Q-filter and the specific parameters of the VCM motor.

B. CALCULATION OF γ

According to (5), $\Delta W(s)$ is re-computed as

$$\Delta W(s) = \frac{\Delta L s + \Delta R}{L s + R}, \tag{20}$$

where $\Delta L = L_n - L$ and $\Delta R = R_n - R$.

Lemma 2:

$$\Delta W(s) \leq \max(\left|\frac{\Delta L}{L}\right|, \left|\frac{\Delta R}{R}\right|). \tag{21}$$

Proof:

According to (20), $|\Delta W(s)|$ is computed as:

$$|\Delta W(j\omega)| = \left|\frac{L\Delta L\omega^2 + R\Delta R}{L^2\omega + R^2} + \frac{(\Delta L R - L\Delta R)}{L^2\omega + R^2} j\omega\right|. \tag{22}$$

1) If

$$\left|\frac{\Delta L}{L}\right| > \left|\frac{\Delta R}{R}\right|, \tag{23}$$

then

$$\left|\frac{\Delta L}{L}\right|^2 - |\Delta W(j\omega)|^2 = \frac{\Delta L^2 R^2 - L^2 \Delta R^2}{L^4\omega^2 + L^2 R^2} > 0. \tag{24}$$

So we have

$$|\Delta W(j\omega)| < \left|\frac{\Delta L}{L}\right| \Big|_{\left|\frac{\Delta L}{L}\right| > \left|\frac{\Delta R}{R}\right|}. \tag{25}$$

2) If

$$\left|\frac{\Delta L}{L}\right| \leq \left|\frac{\Delta R}{R}\right|, \tag{26}$$

then

$$\left|\frac{\Delta R}{R}\right|^2 - |\Delta W(j\omega)|^2 = \frac{(L^2\Delta R^2 - \Delta L^2 R^2)\omega^2}{R^2} \geq 0. \tag{27}$$

So

$$|\Delta W(j\omega)| \leq \left|\frac{\Delta R}{R}\right| \Big|_{\left|\frac{\Delta L}{L}\right| \leq \left|\frac{\Delta R}{R}\right|}. \tag{28}$$

Equation (25) and (28) can be summarized as

$$\begin{cases} \Delta W(j\omega) < \left|\frac{\Delta L}{L}\right| & \left|\frac{\Delta L}{L}\right| > \left|\frac{\Delta R}{R}\right| \\ \Delta W(j\omega) \leq \left|\frac{\Delta R}{R}\right| & \left|\frac{\Delta L}{L}\right| \leq \left|\frac{\Delta R}{R}\right|. \end{cases} \tag{29}$$

Therefore, Lemma 2 is proved.

According to Lemma 2, since γ represent the upper bound of $|\Delta W(j\omega)|$ considering the uncertainties of L and R, γ is calculated as:

$$\gamma = \max(\left\|\frac{\Delta L}{L}\right\|_\infty, \left\|\frac{\Delta R}{R}\right\|_\infty). \tag{30}$$

According to Lemma 1 and (30), the sufficient conditions for the robust stability are presented as:

Conclusion 1: Under Assumption 1, the current control system of VCM motor based on DOB framework is robustly stable if the following conditions hold.

1) $1 + P_n C$ is Hurwitz;

2) $\|Q_T\|_\infty < 1/\max(\|\frac{\Delta L}{L}\|_\infty, \|\frac{\Delta R}{R}\|_\infty)$.

Therefore, the relationship between $\|Q_T\|_\infty$ and specific parameters of the VCM are estabished. Consider the range of L and R is acquirable and $\|Q_T\|_\infty$ can be computed by easily by tools such as MATLAB, it is very convenience to judge the system stability.

According to Conclusion 1, the design guidelines of the DOB framework can be summarized as follow to ensure the robust stability of the VCM current.

Step 1): Make it clearly the range of L and R. The range should be able to cover the practical uncertainties of L and R. Then select a $P_n(s)$ in the range;

Step 2): Design the performance controller $C(s)$ by considering the selected $P_n(s)$ as the plant of the outer-loop. The current characteristic of the DOB control system is decided by $C(s)$ and $P_n(s)$ according to (10). Moreover, make sure that $1+P_nC$ is Hurwitz to satisfy the condition 1) of the sufficient condition. Therefore, the design of $C(s)$ is actually the same with the traditional closed-loop PID control in which $P_n(s)$ is the plant.

Step 3): Calculate the upper bound of the uncertainties according to (30). Choose an design of Q-filter which provide enough robustness and disturbance rejection ability to the disturbance caused by the back-EMF (Since there have been a lot of research on the design of Q-filter in previous work, it is not discussed again in this paper). Calculate $\|Q_T\|_\infty$

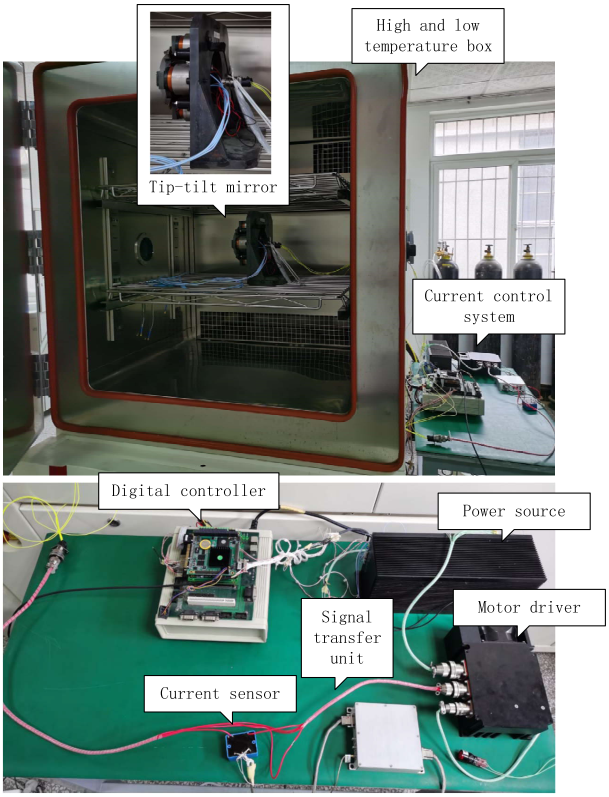

FIGURE 6. **Experiment Setups.**

according to (16). If the Condition 2) of the Conclusion 1 is satisfied, the DOB control system is robustly stable.

V. DESIGN DETAILS AND EXPERIMENTS

In this section, the proposed DOB control method is compared with the traditional PID control on the current control of the VCM in the tip-tilt mirror under different environment temperatures. Both the current characteristic and robustness are investigated when the two different control methods are applied.

The experiment setups are shown in Fig. 6. The tip-tilt mirror is put in a high and low temperature box, which control the environment temperature of the tip-tilt mirror to change from $-40°C$ to $125°C$. The tip-tilt mirror is stored over 3 hours before tested under different temperatures to ensure that the temperature of the mirror is the same with the environment. The current control system consists of motor driver, digital controller, current sensor and signal transfer unit. The current control system is out of the high and low temperature box, so they are not influenced by the temperature changing to ensure the accuracy of the experiment.

A. RESULTS OF TRADITIONAL PID CONTROL

The control system of traditional PID control is shown in Fig. 7. The phase delay and oscillation can be reduced

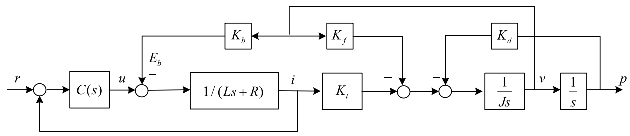

FIGURE 7. **Block diagram of traditional PID current control of the VCM in the tip-tilt mirror.**

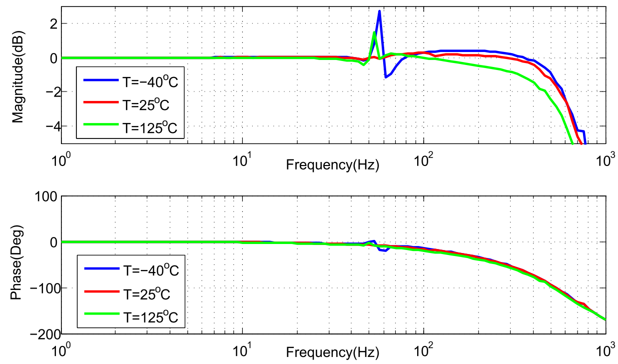

FIGURE 8. **Experiment results of closed-loop current characteristic of the VCM under different environment temperatures based on PID control. The *C*(*s*) is the same under different temperatures.**

through pole-zero elimination, thus $C(s)$ can be set as:

$$C(s) = \frac{K}{s} \cdot \frac{(s + a_0)}{\tau_0 s + 1} \cdot \frac{a_1 s^2 + a_2 s + a_3}{Js^2 + K_f s + K_d}, \tag{31}$$

where K is the controller gain. $\tau_0 > 0$ is the time constant much smaller than $1/a_0$.

In the experiment, $C(s)$ is designed according to the open-loop current characteristic when the temperature is $25°C$, which is

$$C_{PID}(s) = 780\frac{0.00104s + 1}{s(0.0002s + 1)} \frac{8.65e^{-6}s^2 + 8.47e^{-4}s + 1}{9.76e^{-6}s^2 + 1.63e^{-4}s + 1}. \tag{32}$$

In Fig. 8, it is shown that though the current is well compensated when $T = 25°C$, the current performance declined obviously as the temperature changes. Therefore, the traditional current control method cannot provide enough robustness against the uncertainties.

B. RESULTS OF PROPOSED METHODOLOGY

The control system of the proposed DOB method is shown in Fig. 5. Table. 1 shows the parameters of the VCM motor under different environment temperatures. It is shown that $L_1 = 4.7mH$, $L_2 = 5.8mH$, $R_1 = 3.7\Omega$, $R_2 = 7.7\Omega$, which regulate the range of the uncertainties. It is reasonable to select $P_n(s)$ according to the test results under $25°C$, so $L_n = 5.2mH$ and $R_n = 5.4\Omega$. Consider the ratio k between the real current and the feedback signal, then we have

$$\bar{P}_n(s) = \frac{5.4}{0.00096s + 1}, \tag{33}$$

where $\bar{P}_n(s) = kP_n(s)$.

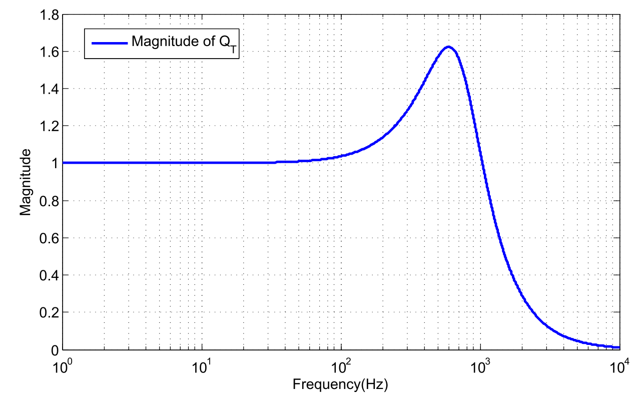

FIGURE 9. Calculation of $|Q_T(s)|$.

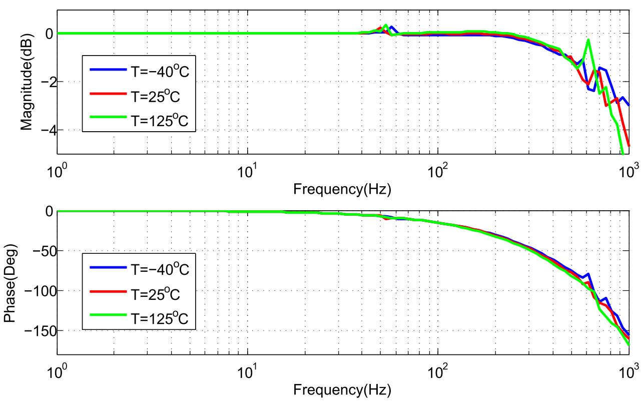

FIGURE 10. Experiment results of the current characteristic under different environment temperatures based on the proposed DOB control method. All parameters designed are the same under different temperatures.

TABLE 1. Parameters of the voice coil motor under different environment temperatures.

Temperature	$-40°C$	$-10°C$	$25°C$	$60°C$	$90°C$	$125°C$
L(mH)	4.7	4.9	5.2	5.3	5.6	5.8
$R(\Omega)$	3.7	4.1	5.4	6.1	6.4	7.6

To design the current performance similar with the PID control under $25°C$, the performance controller $C(s)$ is designed as:

$$C_{DOB}(s) = 790\frac{0.00096s + 1}{s(0.0002s + 1)}. \tag{34}$$

To suppress the disturbance caused by the back-EMF and provide enough robustness, the Q-filter is designed as

$$Q(s) = \frac{1}{(0.0002s + 1)^2}. \tag{35}$$

According to (16), $\|Q_T(s)\|_\infty$ is computed as:

$$Q_T(s) = \frac{4266 + s/(0.0002s + 1)}{4266 + s(0.0002s + 1)}, \tag{36}$$

the magnitude of which is shown in Fig. 9. Thus $\|Q_T(s)\|_\infty = 1.61$. It can also be computed that $\gamma = 0.59$ according to (30). Since $\|Q_T(s)\|_\infty < 1/\gamma$, the system is robustly stable according to Conclusion 1.

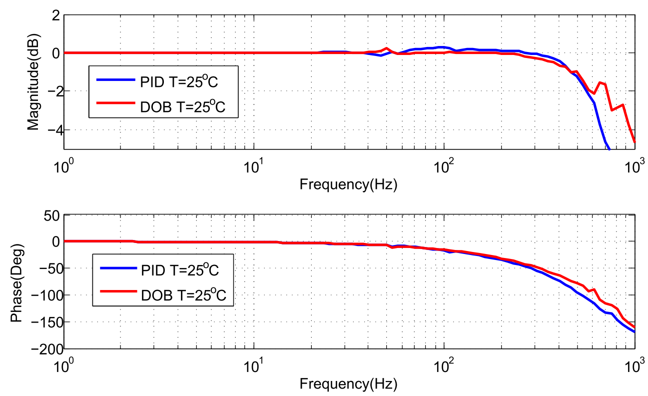

FIGURE 11. Comparison of current characteristic between the traditional PID control and proposed DOB control method. The environment temperature is 25°*C*.

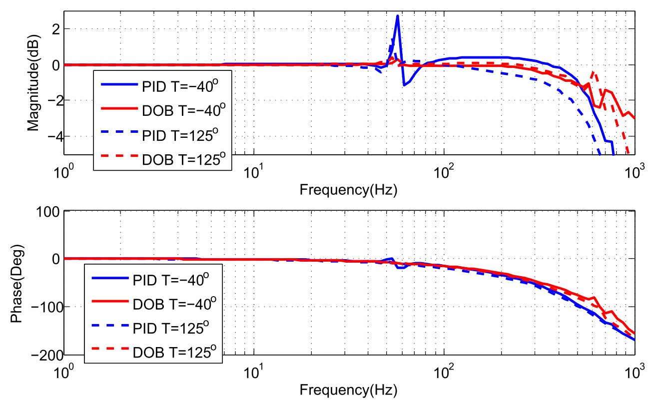

FIGURE 12. Comparison of current characteristic between the traditional PID control and proposed DOB control method. The environment temperatures are −40°*C* and 125°*C*.

Experiment results in Fig. 10 shows that the oscillation and the phase delay of the open-loop current characteristic of the VCM are well compensated by the proposed DOB control method. As the environment temperature changes, the current performance maintains almost the same under the proposed methodology. It should be mentioned that there are some irregularities after 600Hz in Bode plot of the DOB control, which are caused by the measurement noises in the control system.

Fig. 11 and Fig. 12 show that when the environment temperature is 25°C, the current performance of the traditional PID control and proposed DOB control is similar. However, as the temperature changes, the traditional PID control fails to suppress the oscillation, and the dynamics of the current deteriorates obviously. To the contrast, the current performance of proposed DOB control method maintains well. It should to be mentioned that the gain of the PID controller cannot be increased to present the system from "overshoot". Thus the robustness and the control performance of the traditional PID system cannot be improved further. Therefore, the experiment results proof the validity of the proposed control method based on DOB framework.

VI. CONCLUSION

While the current characteristic of the VCM in tip-tilt mirror can be improved by the traditional PID control, the control performance deteriorates obviously under different environment temperature because of the uncertainties of the plant. To solve the problem, the robust control method based on DOB framework is proposed in this paper. By consider the back-EMF as the disturbance on control voltage, the plant model of the control system is simplified. New sufficient conditions for the robust stability are also presented. Compared with the previous work, the upper bound of the uncertainties is calculated in this paper, and the relationship between Q-filter and the electrical parameters of the VCM is established. Therefore, the new sufficient conditions are very convenient for practical application. Experiment results show that as the environment temperature changes, the robustness of the current control is highly improved by the proposed methodology comparing with the traditional PID control.

REFERENCES

[1] T. Tang, S. Niu, X. Chen, and B. Qi, "Disturbance observer-based control of tip-tilt mirror for mitigating telescope vibrations," *IEEE Trans. Instrum. Meas.*, vol. 68, no. 8, pp. 2785–2791, Aug. 2019.

[2] T. Tang, T. Yang, B. Qi, G. Ren, and Q. L. Bao, "Error-based feedforward control for a charge-coupled device tracking system," *IEEE Trans. Ind. Electron.*, vol. 66, no. 10, pp. 8172–8180, Oct. 2019.

[3] C. Luo, J. Sun, X. Wang, and Q. Shen, "Design of voice coil motor with the forward winding for linear vibro-impact systems," *IEEE Trans. Magn.*, vol. 53, no. 8, pp. 1–9, Aug. 2017.

[4] K. J. Smith, D. J. Graham, and J. A. Neasham, "Design and optimization of a voice coil motor with a rotary actuator for an ultrasound scanner," *IEEE Trans. Ind. Electron.*, vol. 62, no. 11, pp. 7073–7078, Nov. 2015.

[5] C.-L. Hsieh and C.-S. Liu, "Design of a voice coil motor actuator with L-Shape coils for optical zooming smartphone cameras," *IEEE Access*, vol. 8, pp. 20884–20891, 2020.

[6] D.-J. Lee and J. Ha Kim, "Integrated design method of multi-axis VCM actuators based on coupled-field-analysis of electro-magnetics and structure," *IEEE Trans. Magn.*, vol. 45, no. 5, pp. 2340–2343, May 2009.

[7] S. Wu, Z. Jiao, L. Yan, R. Zhang, J. Yu, and C.-Y. Chen, "Development of a direct-drive servo valve with high-frequency voice coil motor and advanced digital controller," *IEEE/ASME Trans. Mechatronics*, vol. 19, no. 3, pp. 932–942, Jun. 2014.

[8] H. Guo, D. Wang, and J. Xu, "Research on a high-frequency response direct drive valve system based on voice coil motor," *IEEE Trans. Power Electron.*, vol. 28, no. 5, pp. 2483–2492, May 2013.

[9] Y. Li, M. Chen, L. Cai, and Q. Wu, "Resilient control based on disturbance observer for nonlinear singular stochastic hybrid system with partly unknown Markovian jump parameters," *J. Franklin Inst.*, vol. 355, no. 5, pp. 2243–2265, Mar. 2018.

[10] J. Wang, C. Shao, and Y.-Q. Chen, "Fractional order sliding mode control via disturbance observer for a class of fractional order systems with mismatched disturbance," *Mechatronics*, vol. 53, pp. 8–19, Aug. 2018.

[11] Z. Peng and J. Wang, "Output-feedback path-following control of autonomous underwater vehicles based on an extended state observer and projection neural networks," *IEEE Trans. Syst., Man, Cybern. Syst.*, vol. 48, no. 4, pp. 535–544, Apr. 2018.

[12] H. T. Nguyen and J.-W. Jung, "Disturbance-rejection-based model predictive control: Flexible-mode design with a modulator for three-phase inverters," *IEEE Trans. Ind. Electron.*, vol. 65, no. 4, pp. 2893–2903, Apr. 2018.

[13] E. Sariyildiz and K. Ohnishi, "Stability and robustness of disturbance-observer-based motion control systems," *IEEE Trans. Ind. Electron.*, vol. 62, no. 1, pp. 414–422, Jan. 2015.

[14] E. Sariyildiz, H. Sekiguchi, T. Nozaki, B. Ugurlu, and K. Ohnishi, "A stability analysis for the acceleration-based robust position control of robot manipulators via disturbance observer," *IEEE/ASME Trans. Mechatronics*, vol. 23, no. 5, pp. 2369–2378, Oct. 2018.

[15] E. Sariyildiz and K. Ohnishi, "A guide to design disturbance observer," *J. Dyn. Syst., Meas., Control*, vol. 136, no. 2, Mar. 2014.

[16] E. Sariyildiz, G. Chen, and H. Yu, "A unified robust motion controller design for series elastic actuators," *IEEE/ASME Trans. Mechatronics*, vol. 22, no. 5, pp. 2229–2240, Oct. 2017.

[17] C. Wang, X. Li, L. Guo, and Y. W. Li, "A nonlinear-disturbance-observer-based DC-bus voltage control for a hybrid AC/DC microgrid," *IEEE Trans. Power Electron.*, vol. 29, no. 11, pp. 6162–6177, Nov. 2014.

[18] Z. Wu, T. He, D. Li, Y. Xue, L. Sun, and L. Sun, "Superheated steam temperature control based on modified active disturbance rejection control," *Control Eng. Pract.*, vol. 83, pp. 83–97, Feb. 2019.

[19] H.-S. Kim, H.-T. Moon, and M.-J. Youn, "On-line dead-time compensation method using disturbance observer," *IEEE Trans. Power Electron.*, vol. 18, no. 6, pp. 1336–1345, Nov. 2003.

[20] J. Liu, W. Wu, H. S.-H. Chung, and F. Blaabjerg, "Disturbance observer-based adaptive current control with self-learning ability to improve the grid-injected current for *LCL*-filtered grid-connected inverter," *IEEE Access*, vol. 7, pp. 105376–105390, 2019.

[21] Y. Kim, K.-S. Kim, and S. Kim, "A novel disturbance observer based robust current-control for a PMSM drive system," in *Proc. 54th IEEE Conf. Decis. Control (CDC)*, Osaka, Japan, Dec. 2015, pp. 6043–6046.

[22] O. Wallscheid and E. F. B. Ngoumtsa, "Investigation of disturbance observers for model predictive current control in electric drives," *IEEE Trans. Power Electron.*, vol. 35, no. 12, pp. 13563–13572, Dec. 2020.

[23] L. Wang, J. Mishra, Y. Zhu, and X. Yu, "An improved sliding-mode current control of induction machine in presence of voltage constraints," *IEEE Trans. Ind. Informat.*, vol. 16, no. 2, pp. 1182–1191, Feb. 2020.

[24] W. Xie, "High frequency measurement noise rejection based on disturbance observer," *J. Franklin Inst.*, vol. 347, no. 10, pp. 1825–1836, Dec. 2010. [Online]. Available: http://www.sciencedirect.com/science/article/pii/S0016003210002292

[25] E. Sariyildiz, R. Oboe, and K. Ohnishi, "Disturbance observer-based robust control and its applications: 35th anniversary overview," *IEEE Trans. Ind. Electron.*, vol. 67, no. 3, pp. 2042–2053, Mar. 2020.

[26] J. Su, L. Wang, and J. N. Yun, "A design of disturbance observer in standard H-∞ control framework," *Int. J. Robust Nonlinear Control*, vol. 25, no. 16, pp. 2894–2910, Nov. 2015.

[27] T. Mita, M. Hirata, K. Murata, and H. Zhang, "H_∞ control versus disturbance-observer-based control," *IEEE Trans. Ind. Electron.*, vol. 45, no. 3, pp. 488–495, Jun. 1998.

[28] B. Keun Kim and W. Kyun Chung, "Advanced disturbance observer design for mechanical positioning systems," *IEEE Trans. Ind. Electron.*, vol. 50, no. 6, pp. 1207–1216, Dec. 2003.

[29] Y. Choi, K. Yang, W. Kyun Chung, H. Rok Kim, and I. H. Suh, "On the robustness and performance of disturbance observers for second-order systems," *IEEE Trans. Autom. Control*, vol. 48, no. 2, pp. 315–320, Feb. 2003.

[30] K. Yang, Y. Choi, and W. K. Chung, "On the tracking performance improvement of optical disk drive servo systems using error-based disturbance observer," *IEEE Trans. Ind. Electron.*, vol. 52, no. 1, pp. 270–279, Feb. 2005.

ZONGQI NING received the B.S. and M.S. degrees from the University of Electronic Science and Technology of China, in 2011, both in electronics science and technology. He is currently pursuing the Ph.D. degree in signal processing with the Institute of Optics and Electronics, Chinese Academy of Sciences. Since 2013, he has been working with the Institute of Optics and Electronics, Chinese Academy of Sciences. His current research interests include laser communication, object detection, and tracking.

YAO MAO (Member, IEEE) received the B.S. degree from the Department of Automation, Chongqing University, China, in 2001, and the Ph.D. degree from the Institute of Optics and Electronics, Chinese Academy of Sciences, in 2012. Since 2016, he has been a Professor with the University of Chinese Academy of Sciences. He has published more than 60 papers in refereed conferences and journals. His research interests include information fusion, motion control, object detection, and tracking. He received the Distinguished Scientific Achievement Award from the Chinese Academy of Sciences in 2011.

YONGMEI HUANG received the B.S. degree from the Department of Automation, University of Electronic Science and Technology of China, in 1989, and the Ph.D. degree from the Institute of Optics and Electronics, Chinese Academy of Sciences, in 2005. Since 2005, she has been a Professor with the University of Chinese Academy of Sciences. She has published more than 60 papers in refereed conferences and journals. Her research interests include quantum teleportation, laser communication, object detection, and tracking. She received the Distinguished Scientific Achievement Award twice from the Chinese Academy of Sciences in 2011 and 2019.

CHUNMING GAO received the Ph.D. degree from the School of Electronic Science and Engineering, Nanjing University, in 2004. He is currently a Professor with the University of Electronic Science and Technology of China. He has published more than 50 papers in refereed conferences and journals. His research interests include non-destructive testing based on photo acoustic and optical information and the technology and development of machine vision, machine tactile sensation, and machine audition.